BJRS

BRAZILIAN JOURNAL
OF
RADIATION SCIENCES
07-02A (2019) 01-12

Reproduction of a left-breast 3DCRT field-in-field radiation therapy planning in an anthropomorphic and anthropometric phantom

L. B. Nogueira[a]; J. M. Geraldo[a,b]; C. Barsanelli[b]; J. C. Aquino[c]; and T. P. R. Campos[c]

[a] *Universidade Federal de Minas Gerais / Departamento de Anatomia e Imagem, 30130-100,*

[b] *Hospital Luxemburgo- Instituto Mário Penna, 30380-472,*

[c] *Universidade Federal de Minas Gerais /Departamento de Engenharia Nuclear, 31270-901,*

Belo Horizonte, Minas Gerais, Brasil

lucibn19@yahoo.com.br

ABSTRACT

The proposal of this study was to reproduce the dosimetry plan from a treatment planning system (TPS) following a 3D conformational radiation therapy (3DCRT) protocol of two parallel-opposite fields with the complementary use of the field-in-field technique, applied to a left-breast in a thorax phantom. The computed tomography (CT) images of the thorax phantom were transferred to the XiO version-5 for the elaboration of the breast teletherapeutic planning with 2 Gy per day, in 25 fractions, with prescribed dose of 50 Gy. A set of ten EBT2 radiochromic films were irradiated for calibration. The values of RGB (Red, Green, Blue) of the films were generated and data transformed in optical density (OD). Calibration curve of dose versus OD was elaborated. Radiochromic films were positioned outside and inside of the thorax phantom. Phantom was radiated at the linear accelerator 6 MV Elekta Precise. The intensities in RGB of the films were measured by software ImageJ, transformed in OD and converted in bidimensional dose distributions, applying the calibration curve. In addition, graphics and dose-volume histograms (DVH) were developed. The dose measurements in the glandular- tissue-equivalent (TE) in breast did not present statistically significant differences in relation to values at similar positions generated in the TPS. The organs at risk (OAR's) received doses below the reference val-

ISSN: 2319-0612
Accept Submission 2019-01-03

ues, according to TPS. It was possible to reproduce the dosimetry prescribed in TPS into the thorax phantom exposed to breast conformational radiation therapy. The use of the radiochromic films in dosimetry proves to be increasingly useful and shall become routine in radiotherapy services.

Keywords: breast teletherapy, breast phantom, dosimetry.

1. INTRODUCTION

According to the estimate of the breast cancer incidence in Brazil 2016-2017, conducted by the National Cancer Institute (INCA) together with the Ministry of Health (MOH), the number of new cases of breast malignancy is going to be 57.960 with an estimated risk of 56.20 cases per 100.000 women [1].

Radiation therapy (RT) is one of the treatment methods that delivers a lethal dose on the tumor, sparing healthy tissues from the harmful effects of radiation [2,3]. The modalities often used in breast radiation therapy (breast-RT) involve megavoltage teletherapy, cobalt therapy, electron therapy and high-dose (HDR) brachytherapy by iridium-192 wires [4,5]. New equipment and technologies are in constant development, in order to decrease the dose received by the organs at risk (OARs) and to increase the precision of the dose in the target volume. Thus, the breast radiotherapy can use different planning techniques, such as, conventional 3D or 3D field-in- field [6]. Radiological images (RI) play an important role in the initial tumor's detection and, staging. Also, RI becomes essential to monitoring the treatment progress [7]. Advances in medical imaging have made possible an early diagnosis of breast cancer (CA). Early diagnosis of CA transformed the breast oncology surgery reducing the number of radical mastectomies replacing by conservative procedures. In addition, conservative surgery is followed by radiation therapy at the earliest stage of the disease [8, 9].

Rigorous evaluation of the doses received in the tumor and neighboring tissues is necessary to ensure the efficacy of the treatment. Phantoms are physical objects or mathematical models often applied to reproduce the absorption and scattering radiation in the whole body or part of them, exposed to irradiation fields [9].

A dosimetry study consists in determining the amount of the absorbed dose and its spatial distribution in various parts of the human body, provided by internal or external radiation sources [3]. Studies with radiochromic films in RT dosimetry are expanding due to the equivalence of the effective atomic number and of the mass density with the human tissue, the high spatial resolution, the appropriate dose linearity, the low energy dependence, the insensitivity to visible light and no need for revelation [11, 12, 5]. It has been often used in quality control procedures in radiation therapy. The

validation of breast-RT protocols, generated by the treatment planning systems (TPS), can be assessed through experimental dosimetry.

These protocols include different planning techniques used for the planning of breast cancer treatments, such as conventional conformational 3D and 3D field-in-field. Dosimetric studies with radiochromic films for different treatment techniques are important for the experimental evaluation of these protocols. Reasons to investigate breast-RT dosimetry is due to the high incidence of the disease and its significant rates of recurrence and morbidity associated with the current therapeutic methods. Thus, it is necessary to review and validate the dosimetry of the radiotherapeutic protocols considering the high heterogeneity of the breast region as well as the possible exposition received in the OAR's.

2. MATERIALS AND METHODS

2.1. Thorax and breast phantom, computed tomography (CT) and breast radiation therapy Planning

For the dosimetric reproduction of the breast radiation therapy planning, a thorax and mobile breast phantom was used, developed by the research group NRI / PCTN / UFMG [13, 14], shown in Figure 1.

Figure 1: *Thorax phantom and mobile breast.*

The breast phantom consists of the following tissue-equivalent (TE): glandular-TE, adipose-TE and skin-TE; and the thorax phantom presents the lungs-TE, heart-TE, muscle-TE and bone structure-TE. All these TEs were developed according to the elemental composition of the human body [15].

A Siemens Spirit Syngo CT 200 from the Radiotherapy Service of the Luxemburgo Hospital / Mário Penna Institute, in Belo Horizonte, was used to generate the radiological images, with a protocol of 130 kV and 110 mAs; and slide thickness of 3 mm. Cross-reference marks were made on the thorax phantom to help locating the isocenter.

The CT images were transferred to the XiO version 5.00 planning system for elaborating the breast-RT planning with a typical prescription of total dose of 50 Gy in 25 fractions of 2.0 Gy per day. Two parallel-opposed tangential fields were set, delimited to the breast region, in order to expose little as possible the contralateral breast, lung and heart volumes. The presence of multi-leaf collimators allowed to set more two field-in-field subfields. The subfield format was chosen so as to ensure a better dose uniformity in the left-breast, avoiding the drawbacks of using wedge filters, such as contamination and hardening of the beam, higher monitor dose and larger scattered radiation.

Dose-Volume Histogram (DVH) analysis and isodose curves were performed. The lung and heart region were included in the TPS as OAR's. The parameters for breast radiation therapy planning were shown in Table 1.

Table 1: Radiation therapy planning parameters for left breast phantom.

	Internal field 1 / Infield internal 2	**External field 1/ Infield external 2**
Technique	Isocentric	Isocentric
Gantry angle (deg)	305 º/ 305 º	130 º / 130 º
Fields (cm)	x1= 5.5; x2= 6.5/ x1= 5.5; x2= 4.9. y1= 8.0; y2= 7.6/ y1= 8.0; y2= 7.6.	x1= 7.3; x2= 5.5/ x1= 5.6; x2= 5.5. y1= 8.2; y2= 7.9/ y1= 8.2; y2= 7.9.
Weight (Gy)	28.5/ 1.5	19.5/ 0.5
MU (monitor unit)	120.0 / 6.4	91.4/ 2.4

2.2 Positioning of radiochromic films and irradiation of breast phantom

Gafchromic® EBT2-type, from International Specialty Products (ISP) [16], was used in the dosimetry studies. Five radiochromic films were cut in compatible dimensions with the anatomy of the left-breast phantom, positioned inside the breast glandular-TE with spacing of 2-cm each, following the orientation of the transverse plane of the human body, as shown in Figure 2 (A). Two other radiochromic films of 5 x 7 cm were placed inside in the thorax phantom, one in the right-lung-TE and the other in the left-lung-TE, approximately 4.5-cm deep, following the orientation of the coronal plane of the human body. A radiochromic film with dimensions of 7 x 11 cm was positioned on the upper face of the heart-TE, following the coronal plane of the human body. Another film of 10 x 10 cm was placed in the posterior-breast glandular-TE (region near of the pectoralis major muscle), following the orientation of the coronal plane of the thorax phantom, as shown in Figure 2 (A). Four radiochromic films of 2 x 3 cm were placed in the skin-TE on the left-breast, following the orientation of the coronal plane of the thorax phantom. All radiochromic films were sealed with plastic to protect against external agents.

At the exposure time, the thorax phantom was placed on a radio-transparent support on the radiotherapy table, so that the radiation beam was out of the support. The reference marks on the skin-TE were used for positioning the lasers, ensuring the reproducibility of the isocentric positioning in

relation to the fiducial points defined in the TPS. The TPS was reproduced in the linear accelerator, model LINAC Electra Precise 6MV. Figure 2 (B) shows the TPS of the breast-phantom, with indications of CTV1/PTV1 and PTV3; and isodose curves of 107% (blue), 100% (red) and 95% (yellow), usually presented in the planning.

Figure 2: *A) breast phantom (films 1 to 5-transverse orientation and film 6- coronal orientation, following plane of the human body); and B) radiation therapy planning of the breast phantom.*

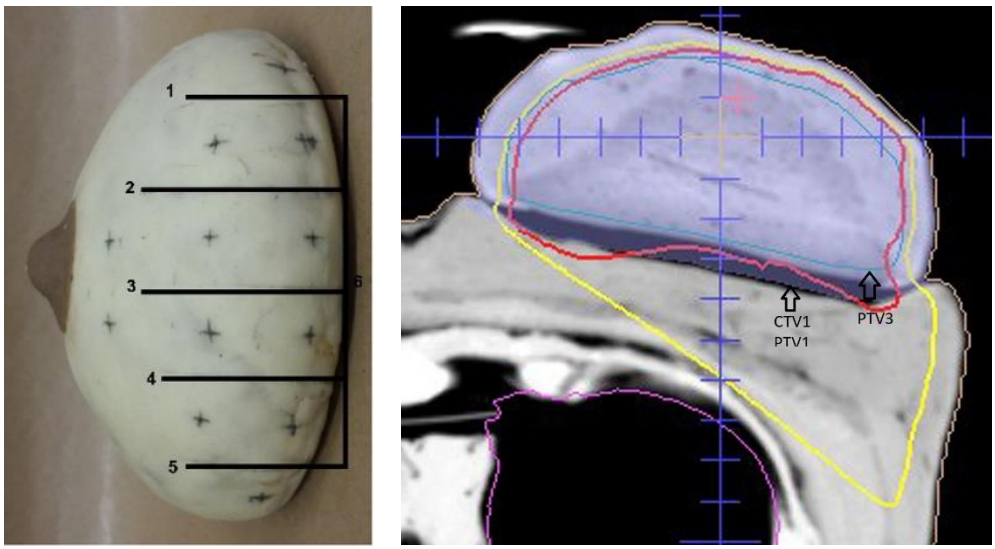

A B

2.3 Calibration and digitization of the radiochromic films

The LINAC accelerator was calibrated following the protocol TRS-398 [17] with a monitor unit of 0.01Gy at the electronic equilibrium depth for a 10 cm x 10 cm field and at a source-skin distance (SSD) of 100 cm.

The calibration was prepared with a set of ten radiochromic films of the Gafchromic® EBT2-type, from International Specialty Products (ISP) [16], with 3.0 x 3.0 cm. They were exposed to doses from 0 to 250 cGy, in intervals of 25 cGy. Those films were placed centralized between two plates of a solid-water phantom, model Gammex 457 with dimensions of 30 x 30 cm of 4-cm thickness,

following the standard setup of LINAC calibration, assuming a Source Axis Distance *(*SAD) of 100 cm and a field of 10 cm x 10 cm.

After 24 h of exposure, the radiochromic films were digitized on the HP Scanjet G 4050 transmission scanner. The image color decomposition was performed and intensities of the color components in RGB (Red, Green, Blue) were obtained. The RGB value of each component is set from 0 to 255, with 255 being the maximum value corresponding to the maximum color intensity and zero being the minimum value corresponding to the absence of the color component. The ImageJ software was used to decompose the digitized images into their RGB components [18].

2.4 Reading of radiochromic films - optical density, standard deviation and dose.

The amount of radiation absorbed in the radiochromic films was defined by the degree of the intensity of the red-component of the digitized image. The calibration curve was adjusted as a function of the absorbed dose versus the optical density from the red-component. The optical density was associated with the intensity of the red-component, as follows:

$$OD = \log_{10} \frac{I_0}{I} \tag{1}$$

in which *OD* is the optical density of the film; I_0 represents the intensity of the R or G components in the non-irradiated film; and I represents the intensity of the R or G components intensity in the irradiated film. The standard deviation of the optical densities of the sensitized and non-sensitized radiochromic films were evaluated as follows:

$$\sigma_{OD}(RGB) = \frac{1}{ln\,(10)} \sqrt{\frac{\sigma_I\,(RGB)^2 + {\sigma_o}^2}{m_I(RGB)^2 - m(FO)^2} + \frac{\sigma_n\,(RGB)^2 + {\sigma_o}^2}{m_n(RGB)^2 - m(FO)^2}} \tag{2}$$

in which σ_{OD} is the standard deviation of the optical density obtained from the intensities of R, G or B components from the film; σ_I is the standard deviation of the averages of the R, G and B components of the irradiated film; σ_o is the standard deviation of a digitized opaque film; σ_n is the standard deviation of the averages of the R, G or B components of the non- irradiated film; m_I is the average of the R, G or B components of the irradiated film; m_n is the average of the R, G, or B components

of the non-irradiated film; and *m(FO*) is the average of the R, G, or B components of the opaque film.

The relation between optical density and dose, in cGy, was obtained by a quadratic non-linear adjustment between the *OD* values, from calibration films, and the doses in cGy, referent to PDP normalized to the maximum dose, following the expression:

$$D = a + b_1.OD + b_2.OD^2 \quad (3)$$

in which *D* represents the measured dose; *a, b_1* and *b_2* curve fitting parameters; and *OD* represents the optical density.

2.5 Experimental dosimetry of radiochromic films

After irradiation of the left breast phantom, the sensitized radiochromic films were removed from the left-breast phantom, stored for 24 h and digitized in the HP Scanjet G4050 scanner.

The digitized images were decomposed into their RGB components in the ImageJ software [18] and ASCII files were generated, representative of the red-component. The data were converted into the optical density, applying Eq.1 to each pixel of the decomposed image and calculated the standard deviation, according to Eq.2. The calibration curve, Eq. 3, was used for the dose evaluation in cGy. The spatial dose distribution was preserved. Optical density values were then converted to dose in cGy and the dose maps were presented as two-dimensional images, reproduced at dose intervals of 0.1 Gy.

The absorbed doses in the EBT2 radiochromic films positioned in the breast glandular-TE, in the posterior breast gland-TE, in the lungs-TE, in the heart-TE and in the skin-TE were analyzed and compared with the absorbed doses calculated by the TPS. These absorbed doses were also compared with dosimetric data from previous studies performed by Nogueira et al. and references as ICRU 50, ICRU 62 and Marks et al. [5, 7, 19, 20, 21, 22].

The DVH generated by the TPS was evaluated for the PTV and the OAR's, such as the lung and the heart. Two PTVs were designed: one involving the breast skin (zero margins) called PTV1 and another with a margin of 7-mm below the skin (PTV3).

3. RESULTS AND DISCUSSION

3.1 Calibration of radiochromic films

Calibration was performed with solid water plates. A set of ten radiochromic films was positioned at a depth of 4 cm, corresponding to 91.1% of the PDP, and exposed to variable monitored units (MU), providing the absorbed doses of: 227.75 cGy; 204.97 cGy; 182.2 cGy; 159.42 cGy; 136.65 cGy; 113.87 cGy; 91.1 cGy; 68.32 cGy; 45.55 cGy; 22.77 cGy; 0cGy.

Figure 3 shows the calibration curve of the dose, in cGy, as a function of the optical density of the red-component, whose mathematical adjustment was obtained in the Origin [23] software.

Figure 3: *Dose (cGy) versus optical density of the red RGB component.*

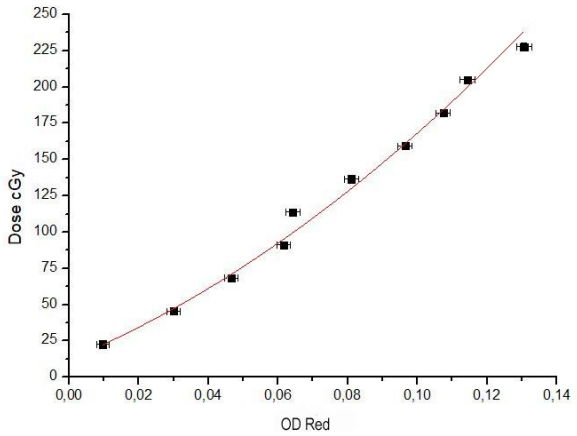

It is observed that the dose increases as the optical density also increases. The standard deviations of the optical density evaluated by Eq.2 were identified, as well as the uncertainties in the PDP measurements. The adjustment of the calibration curve was prepared through the polynomial equation. The quality of the regression was 0.99252 (R^2). The dose uncertainties presented agree with the TPS, which should be less than 2.5%.

The correlation between dose versus optical density satisfied the following polynomial relation:

$$D = 12{,}17717(\pm 2{,}22435) + (1001{,}69451\ (\pm 139{,}32986).OD) + (5589{,}78122\ (\pm 1340{,}84435).OD^2) \quad (3)$$

in which *D* represents the dose, in cGy, and *OD* is the optical density, with a regression quality of 0.99252 (R^2).

3.2 Analysis of the dose-volume histogram (DVH)

Figure 4 shows the DVH of the TPS. The data showed that the minimum dose in PTV3 was 31.33 Gy, maximum dose of 53.27 Gy, total mean dose of 50.99 Gy for one prescribed total dose of 50 Gy in 100% isodose.

On the other hand, for PTV1 the minimum dose was 0.030 Gy, maximum dose of 47.56 Gy and mean dose of 1.71 Gy for the same prescribed total dose of 50 Gy in 100% isodose. Such data demonstrated the need to establish a clinical consensus to define the margins of PTV in the breast treatment. A PTV with borders near to the skin will have an extensive volume under low dose, due to the build-up of the megavoltage beams, leading to different dosimetry results as shown comparing PTV3 to PTV1, with a significant difference in the mean dose.

Figure 4: *Dose-Volume Histogram (DVH) of the breast radiation therapy planning*

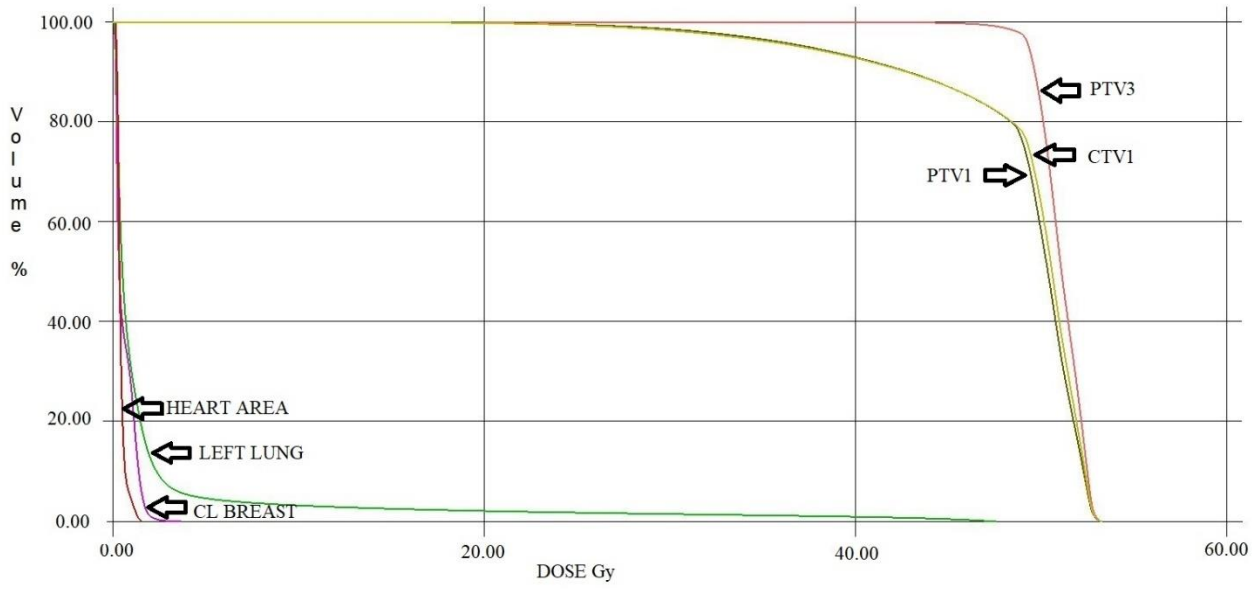

According to the data generated in the DVH, PTV3 received more than 95% of the prescribed dose in 95% of the irradiated volume. It agrees with ICRU 50 and ICRU 62, demonstrating that the plan was adequate. In turn, PTV1 received 95% of the dose in only 40% of its volume, including skin.

The left lung-TE received 20 Gy in a lower volume than 5.00% of the total volume. A limit value of 20 Gy is required in a lower volume than or equal to 30% of the organ volume (V20 ≤ 30%), according to Marks et al. [22]. According to ICRU 62 [20], the dose limits are 30 Gy in a 200 cm^3 of lung tissue. This requirement was also satisfied.

The heart-TE received 25 Gy in a lower volume than 5.0 % of the total heart-volume, following the requirements presented by Marks et al. [22]. The dose limit referent to the total heart volume is 25 Gy, in a lower volume than or equal to 10% of the organ volume (V25 ≤ 10%). According to ICRU 62 [20] dose limits are 30 Gy by volume of 30 cm^3 for the myocardium. These values were also satisfied.

3.3 Dosimetry of radiochromic films in the breast glandular-TE

Figure 5 shows the spatial dose distribution deposited on the a radiochromic film positioned inside the breast glandular-TE, following the orientation of the transverse plane of the human body.

Figure 5: *Dose spatial distribution, in Gy, measured in the radiochromic film 1 in the breast glandular-TE.*

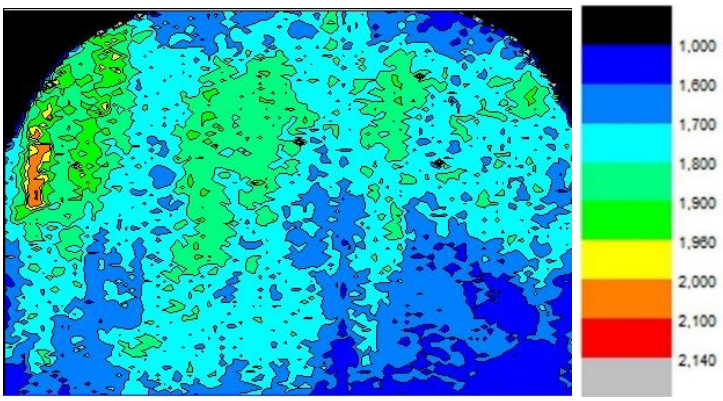

It can be observed that the spatial dose distribution in the film 1, in which the doses were in the ranges of 1.6 to 1.8 Gy, corresponding to between 80% and 90% of the prescribed dose of 2.0 Gy referent to a fraction.

Table 2 shows the absorbed mean doses in the films of the breast glandular-TE, in comparison to the prescribed dose percentage per fraction of 2.0 Gy. The absorbed average doses in radiochromic films, in the glandular-TE, compared to the prescribed dose percentage of 2.0 Gy per fraction was represented in Table 2.

Table 2: absorbed mean doses in the radiochromic films in the breast glandular-TE compared to the prescribed dose percentage of 2.0 Gy per fraction.

Radiochromic films - Breast glandular-TE	**Mean dose – Gy/ Standard deviation**	**Prescribed dose per fraction (%)**
Breast 1	1.72 / 0.17	86.00
Breast 2	1.65 / 0.21	82.50
Breast 3	1.55 / 0.25	77.50
Breast 4	1.68 / 0.23	84.00
Breast 5	1.67 / 0.21	83.50

The absorbed mean dose of the five radiochromic films was 1.65 Gy, corresponding to 81.47 % of the mean dose of the DVH of 2.03 Gy per fraction, and 82.70 % of the prescribed dose of 2.0 Gy per fraction.

According to Nogueira et. al. [5], doses were measured in breast glandular-TE submitted to a conformational two-oppose-parallel breast radiotherapy. The absorbed average doses in the films positioned inside the glandular-TE, following a sagittal plane, were between 1.8 and 1.92 Gy, corresponding to 100% to 106.6% of the prescribed dose of 1.8 Gy per fraction.

The average value of the dose percentage relative to the prescribed dose fraction in this study was lower than the same value in the study done by Nogueira et al. [5]. Indeed, the spatial dose distribution in the film did not follow a homogeneous distribution. One can observe a lower dose at the bottom of the film. It should be due to a small empty space between the removable breast and the thorax wall. Such lack of equilibrium electronic could have reduced the internal dose at the film´s bottom. The mean dose was taken in the whole film; therefore, such fact can contribute to the reduction of the dose percentage of 82% related to the prescribed dose. In Nogueira et al [5], the phantom had a breast fixed on the thorax, which had no space between. And, the present phantom has its synthetic removable breast. Thus, the lower values found in this study can be explained by the positioning of the radiochromic films within the breast phantom, the possible space existing at the bottom of the breast, and the beam orientation in relation to the film plane. However, more studies should be performed.

3.4 Dosimetry of radiochromic films in the posterior breast glandular-TE

Figure 6 (A) shows the spatial distribution of the deposited doses in the radiochromic film positioned in the orientation of the coronal plane of the human body. Figure 6 (B) shows isodose curves in the coronal plane of the breast phantom, region where the radiochromic film was positioned.

Figure 6: *(A) Dose spatial distribution, in Gy, measured in the radiochromic film in the posterior breast glandular-TE and (B) isodose curves in the coronal plane of the breast phantom*

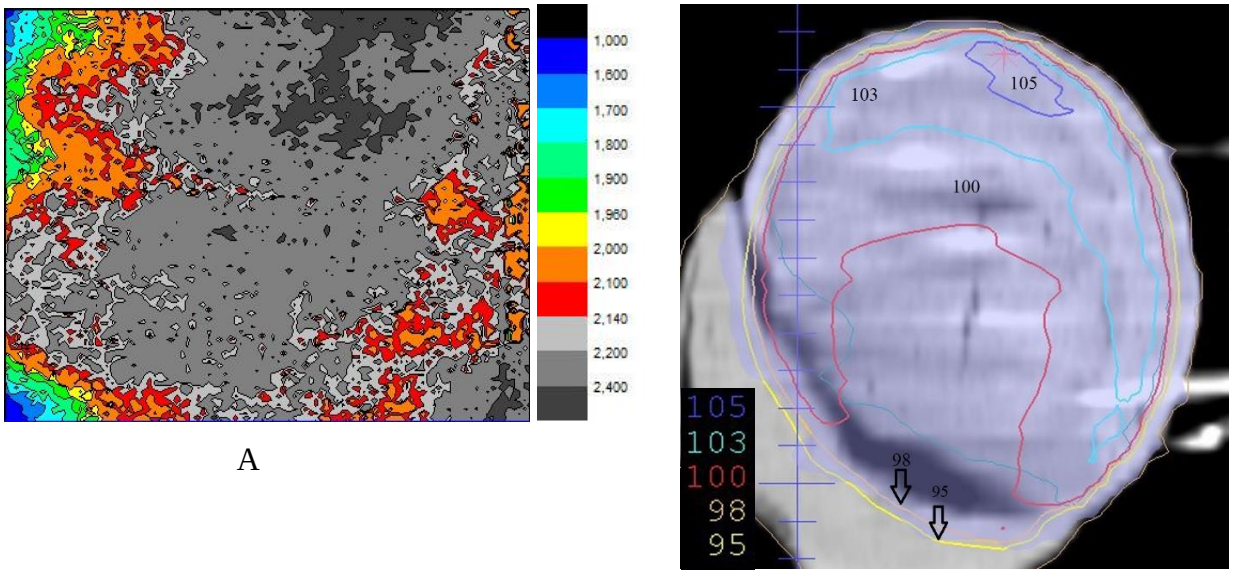

A

B

It can be observed in the posterior breast glandular-TE that the spatial dose distribution was better represented by the radiochromic film positioned inside the breast phantom in the orientation of the coronal plane of the human body, than with the film in the orientation of the transversal plane of the human body. However, further studies on this matter are required.

The mean dose in the posterior breast glandular-TE was 2.21 ± 0.1426 Gy, corresponding to 110 ± 7 % of the prescribed dose of 2.0 Gy. Fig. 6 (B) shows regions with isodose above 100 % of the prescribed dose, which can be correlated with the dose distribution in Fig. 6 (A).

According to Nogueira et. al. [5], glandular-TE doses was found on the breast in the range of 1.5 to 2.2 Gy that corresponded from 85% to 115% of the dose in the radiation therapy planning for a prescribed dose of 1.8 Gy per fraction.

It can be observed that the present measured doses corroborate with the data found by Nogueira et. al. [5]. According to ICRU 50 [21] and 62 [20], the plans are considered adequate when there is coverage of at least 95 % of the PTV for 95 % of the prescribed dose.

3.5 Dosimetry of radiochromic films in the right and left lungs TE's and heart-TE

Figure 7 shows the spatial dose distribution in the films positioned inside the lungs TE's, following the orientation of the coronal plane, as well as the film positioned in the upper face of the heart-TE in the thorax phantom, following the orientation of the coronal plane.

Figure 7: *Dose spatial distribution, in Gy, at (A) right lung-TE, (B) left lung-TE, (C) heart-TE and (D) scale in Gy.*

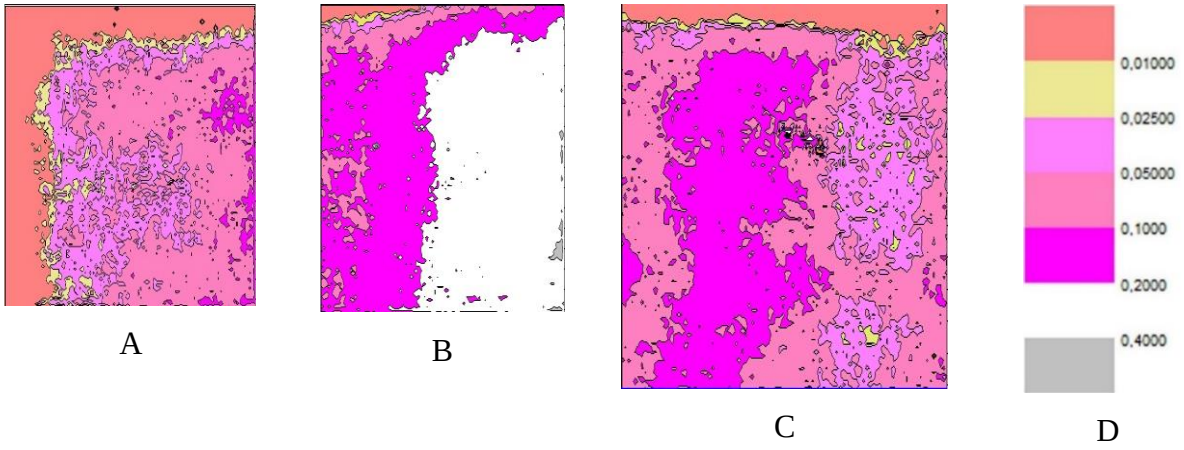

The mean dose in the right-lung-TE was 0.03 ± 0.04 Gy, corresponding to 1.5 ± 2 % of the prescribed dose of 2.0 Gy. The mean dose in the left-lung-TE was 0.19 ± 0.08 Gy, corresponding to 9.5 ± 4 % of the prescribed dose of 2.0 Gy. It can be seen in Figure 7 (A) and (B) that the spatial dose representation is lower than 0.4 Gy. According to Marks et al. [22], the doses in the lungs from breast-RT should be 20 Gy in a lower volume than or equal to 30% of the organ volume (V20 ≤ 30%). According to ICRU 62 [20], dose limits are 30 Gy in volume 200 cm^3 of lung tissue.

The mean dose in the heart-TE was 0.07 ± 0.04 Gy, corresponding to 3.5 ± 2 % of the prescribed dose of 2.0 Gy. It can be seen in Figure 7 (C) that the spatial dose representation is lower than 0.4 Gy of the dose. According to Marks et al. [22], the doses for the heart in radiation therapy planning of the breast should be 25 Gy in lower volume than or equal to 10% of the organ volume (V25 ≤ 10%). According to ICRU 62 [20] the dose limits are 30 Gy in volume 30 cm^3 for the myocardium.

Although the absorbed doses in the radiochromic films do not present the absorbed dose according to the organ volume, they show that the doses measured are well below the doses of tolerances used in the literature. We can note that the dose percentage in left lung-TE was higher relative dose percentages in right lung-TE and heart-TE. This fact is expected because the irradiated breast was the left, closer to the beam.

3.6 Dosimetry of radiochromic films in skin-TE

Figure 8 shows the spatial distribution of the deposited doses in the four radiochromic films positioned in the skin-TE of the breast phantom, following the orientation of the coronal plane of the human body.

Figure 8: *Dose spatial distribution, in Gy, measured in the radiochromic films Skin-TE 1 (A), Skin-TE 2 (B), Skin-TE 3 (C) and Skin-TE 4(D).*

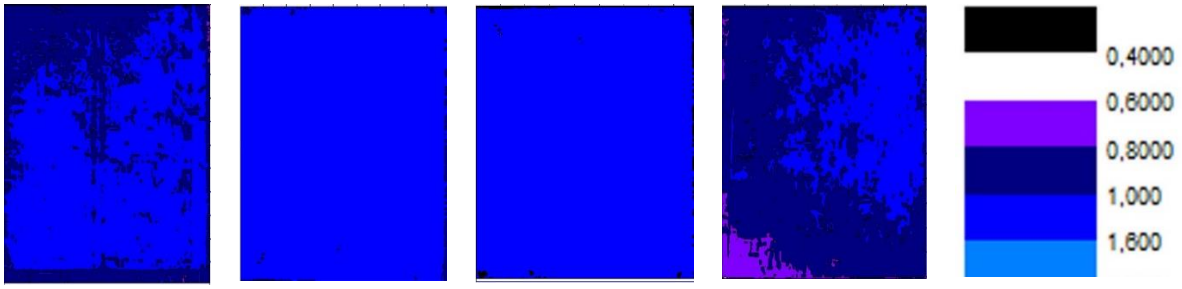

A B C D

The absorbed dose estimate in skin-TE was in the range of 0.6 Gy to 1.0 Gy, with a mean and standard deviation of 1.07 ± 0.01 Gy corresponding to 53.5 ± 0.5 % of the prescribed dose of 2.0 Gy per fraction. The absorbed average doses by the films Skin-TE 1, 2, 3 and 4 were respectively: 1.01 ± 0.05 Gy; 1.18 ± 0.07 Gy, 0.96 ± 0.08 Gy and 1.14 ± 0.08 Gy.

According to Nogueira et. al. [7], in which skin-TE dose was measured following a conventional breast radiation therapy planning, the mean dose and standard deviations were 1.2 ± 0.1Gy, corre-

sponding to 68.5 ± 6 %, 4 of the prescribed dose of 1.8 Gy; and dose of 1.1 ± 0.2 Gy corresponded to 59.3 ± 8.5 % of the prescribed dose of 1.8 Gy.

These results corroborate to demonstrate that the entrance doses on the skin of the patients in treatment of breast radiation therapy are about 50 to 70% of the prescribed dose.

3.7 Analysis of experimental uncertainties

The sources of uncertainties involved in the experiment were estimated according the International Standards Organization (ISO) [24]. The uncertainties of the experimental measurements are difficult to be assessed because of the number of variables involved. The authors estimated a value for the combined experimental uncertainties of ±6% reliability factor K= 2 according to the value recommended by ICRU 24. This value was estimated after analyzing possible sources of uncertainties present in the experiment. This high estimated value is due to the large number of procedures and variables involved, which have not yet been subjected to any process of normalization or standardization.

4. CONCLUSION

The dosimetric reproduction of the breast radiation therapy planning directed in the anthropomorphic and anthropometric breast phantom was viable, even with different planning techniques. The experimental spatial dose distribution presented coherent results, compared to TPS, as well as data from the literature.

5. ACKNOWLEDGMENT

The authors thankful the Luxemburgo Hospital - Mário Penna Institute for conducting the experiment, by project. We are thankful to CNPq due to the REBRAT/SUS, 2013, project. We are thankful to the institutional support from the CAPES, CNPq institutions.

REFERENCES

1. INCA- Instituto Nacional de Câncer**. Estimativa 2016-2017: Incidência de Câncer no Brasil**. Rio de Janeiro, 2015.

2. THOMPSON, L.; DIAS, H. G.; CAMPOS, T. P. R. Dosimetry in brain tumor phantom at 15 MV 3D conformal radiation therapy. **Radiation Oncology (Online)**, v. 8, p.168, 2013.

3. XU, X. G. **Computational phantoms for radiation dosimetry: a 40-Year history of evolution. In Handbook of Anatomical Models for Radiation Dosimetry**, Edited by Xu XG, Eckerman KF, Boca Raton: Taylor & Francis, 2013.

4. HOMMA, L. A. H. **Aspects of the application of sentinel lymph node surgery and complementary brachytherapy in initial invasive breast cancer, Master's Dissertation, Nuclear Engineering Department, Federal University of Minas Gerais**, Brazil, 2005.

5. NOGUEIRA, L. B.; SILVA, H. L. L.; CAMPOS, T. P. R. Experimental dosimetry in conformal breast teletherapy compared with the planning system. **Applied Radiation and Isotopes,** v. 97, p. 93-100, 2015.

6. TRINDADE, C.; SILVA L. P.; MARTINS L. P.; GARCIA, P. L.; SANTOS M. R.; BATISTA, D. V. S.; VIEIRA, A. M. M. T. L.; ROCHA, I. M. Comparison between 3D dynamics filter technique, fiel-in-field, electronic compensator in breast cancer. **Revista Brasileira de Física Médica**, v.6 (3), p. 149-53, 2012.

7. NOGUEIRA, L. B.; SILVA, H. L. L.; SILVA, S. D.; CAMPOS, T. P. R. Skin dosimetry in breast teletherapy on an anthropomorphic and anthropometric phantom. **Austin J Radiol.,** v. 2(4), p.1024, 2015.

8. VOLKER, R..; ABDUL, A.; AZIZ, A. L.; *et al*. Tangential beam IMRT versus tangential beam 3D-CRT of the chest wall in postmastectomy breast cancer patients: a dosimetric comparison. **Radiation Oncology,** v. 6, p. 392-406, 2011.

9. SALVAJOLI, J. V.; SOUHANI, L.; FARIA, S. L. **The Role of Radiotherapy in Cancer Treatment - Advances and Challenges, Radioterapia em oncologia**, 2nd ed, Rio de Janeiro: Medsi Editora Medica e Científica, 2013.

10. Ministry of Health- Ordinance-453 Guidelines for **Radiological Protection in Medical and Dental Radiology**. Secretariat of Sanitary Monitoring, Brazil, 1998.

11. BUTSON, M. J.; CHEUNG, T.; YU, P. K. Radiochromic film dosimetry in water phantoms. **Phys Med Biol.,** v. 46(1), p. 24-31, 2001.

12. AMARAL, L. L.; OLIVEIRA, H. F.; FAIRBANKS, L. R.; NICOLUCCI, NETTO, T.G. Averification methodology for in vivo dosimetry in stereotactic radiotherapy. **Braz.J.Med. Phys,** v.6(3), p. 129–132, 2012.

13. CAMPOS, T. P. R; THOMPSON, L.; NOGUEIRA, L. B.; DUARTE, I. L.; MATOS, A. S.; TEIXEIRA, C. H; et. al. **Anthropomorphic and Anthropometric Simulators of the Structures, Tissues and Organs of the Human Body, Brazil patent BR PI1004465-5**, UFMG, Minas Gerais, Brazil, 2012.

14. SCHETTINI, M. P.; MAIA, M.; CAMPOS, T. P. R. The Development of an anthropomorphic and anthropometric thorax female phantom for experimental radiodosimentry. **Int J Low Radiat**., v. 4, p. 124-135, 2007.

15. ICRU 44- International Commission on Radiation Units and Measurements. **Tissue substitutes in radiation dosimetry and measurement. ICRU Report 44**, Bethesda: ICRU, 1989.

16. ISP. International Specialty Products. **Gatchromic self- developing dosimetry films | EBT2 | EBT 3 | Cyberknife | HD-V2 | MD-V3 | RTQA2 Ashland Inc**. New Jersey: ISP, 2010.

17. IAEA- International Atomic Energy Agency. **Absorbed dose determination in external beam radiotherapy: An Internationa code of practice for dosimetry based on standards of absorbed dose to water.** Vienna: IAEA , 2000.

18. RASBAND, W. S. **ImageJ, U. S. National Institutes of Health**. Bethesda, Maryland, USA. 2011. Available at: <http://imagej.nih.gov/ij/>. Last accessed: jun. 2017.

19. NOGUEIRA, L. B.; CAMPOS, T. P. R. Nuclear characterization and investigation of radio-active bioglass seed surfaces for brachytherapy via scanning electron microscopy. **Journal of Sol-Gel Science and Technology**, v. 58, p. 251 – 258, 2011.

20. ICRU 62- International Commission on Radiation Units. **Prescribing, Recording and Reporting Photon Beam Therapy. ICRU Report 62,** Bethesda: ICRU, 1999.

21. ICRU 50- International Commission on Radiation. **Prescribing, Recording, and Reporting Photon Beam Therapy. ICRU Report 50**, Bethesda: ICRU, 1993.

22. MARKS, L. B.; YORKE, E. D.; JACKSON, A.; TENHAKEN, R. K.; CONSTINE, L. S.; EISBRUCH, A. Use of normal tissue complication probability models in the clinic. **Int.J. Radiat. Oncol. Biol.Phys**, v. 76(3), p. 10–19, 2010.

23. ORIGINLAB: **Origin and OriginPro** - Data analysis and graphing – Origin. Available at: <http://www.originlab.com/> . Last accessed: jun. 2017.

24. ANDRE, P.; BURNS, D.; HOHLFELD, K.; HUQ, M.; KANAI, T.; LAITANO, F.; SMYTH, V.; VYNCKIER, S. Absorbed dose determination in external beam radiotherapy: na international code of practice for dosimetry based on standards of absorbed dose to water. R: IAEA TRS-398**. Int At Energy Agency IAEA**, v.11(b), p.13–181, 2004.